# EXPERIMENTAL INVESTIGATION OF SUPERSONIC TWO-PHASE FLOW OVER BODIES

A. P. Alkhimov, N. I. Nesterovich, and A. N. Papyrin

UDC 532.529

The investigation of two-phase flow over bodies is important in science and engineering in respect of tasks in energy technology, deposition of reinforcing coatings, etc. For example, the presence of fine solid or liquid particles in the carrier gas (or vapor) phase has a considerable effect on the flow parameters near the body and on its aerodynamic characteristics, in the operation of turbines with vapor condensation, in dust detonation and in the motion of aircraft under cloud conditions.

At present there are papers [1-4] which consider some aspects of this problem by solving for the motion of individual particles in the given gas flow. However, a full analysis of two-phase flow over a body is complex because of the diversity of physical processes governing the phenomenon. These are processes connected with the motion of particles in the stagnation region and interaction between them and the body surface, leading in some cases to erosion and ablation of material, and in other cases to implantation of particles into the surface layer and the formation of stable coatings. It is also important to account for factors stemming from the influence of particles on the gas flow field, especially in supersonic flow over bodies.

It should be noted that the experimental papers (see, e.g., [5, 6]) refer mainly to determination of the integral parameters of the body (drag, heat flux, etc.). In order to elucidate and study individual factors influencing the nature of the total process, one must set up experiments to measure local parameters of two-phase flow and observe the dynamic motion of individual particles as they interact with the body. To accomplish such measurements one must employ diagnostic methods affording high spatial and timewise resolution without introducing perturbations into the test flow.

This paper presents some results of an experimental investigation of supersonic two-phase flow over bodies, obtained by high-speed methods of laser diagnostics: the laser-Doppler velocity meter and also a scheme for pulsed visualization in scattered and transmitted light. Data have been obtained on the nature of the change in wave structure near the bodies upon injection of various particles into the flow.

1. The experimental equipment and the diagnostic methods are illustrated in Fig. 1. Particle velocity was measured with the aid of a laser-Doppler velocity meter (LDVM), with a direct spectral method of recording the Doppler frequency shift. The LDVM scheme included the following elements: a single-frequency helium–neon type LG-159 laser 1; a beam splitter plate 2; a 100% reflection mirror 3; a polarizer to record the intensity of the reference ray 4; focusing lenses 5 and 6; the aperture stop of the detector optical system 7; collecting lens 8; matching objective 9; multibeam confocal interferometer with exit photomultiplier 10; oscilloscope 11. Laser-Doppler meters with direct spectral analysis are the most efficient in investigation of high-speed flows ($v \geqslant 10^2$ m/sec). Also, in contrast to the LDVM based on picking out the Doppler signal by means of photomixing, with the schemes used here one can determine both the magnitude and the direction of the velocity. This is important for simultaneous recording of fluxes of particles moving in opposite directions.

We used a pulsed shadowgraph system to investigate the microstructure of the density field. The light source was a ruby laser 1' operating in a modulated regime with a pulse $\tau$ = 30 nsec. Here the displacement of particles during the exposure did not exceed their diameter. The laser light beam was directed by the 100% reflecting mirror 2' to a telescope system consisting of lenses 3' and 5' and the aperture 4'. An image of the test object was formed by the objectives 6' and 7' and recorded by the camera 8'. The change in wave structure with time was studied by taking multiple shadowgraph pictures employing a ruby laser to generate a series of pulses with a given period (a laser stroboscope).

Novosibirsk. Translated from Zhurnal Prikladnoi Mekhaniki Tekhnicheskoi Fiziki, No. 2, pp. 66-74, March-April, 1982. Original article submitted January 14, 1981.

0021-8944/82/2302-0219$07.50  

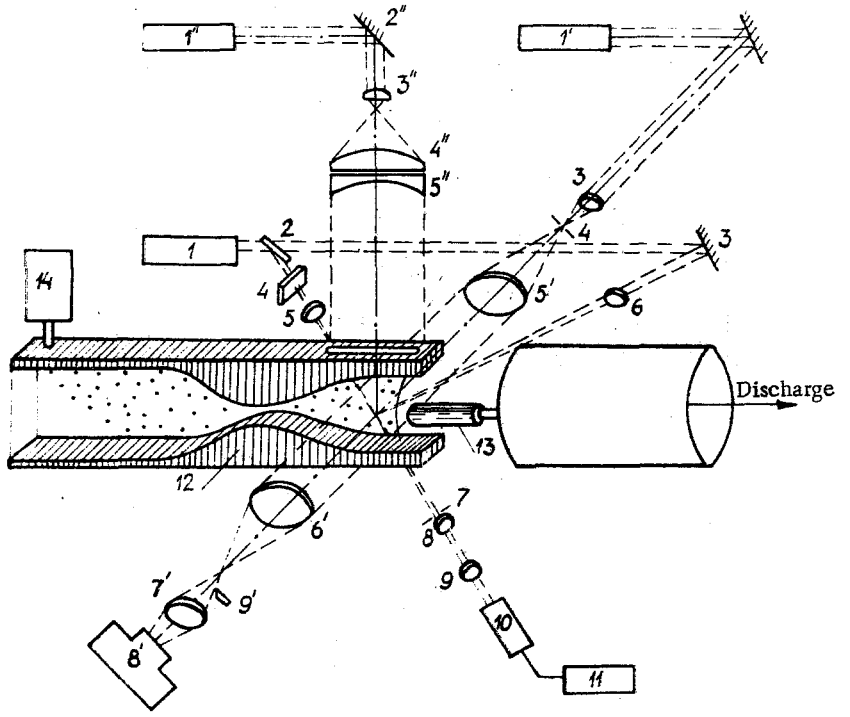


Fig. 1

To observe the particle trajectories we used laser visualization in scattered light (a laser "knife-edge"). The ruby laser 1" operated in the peak lasing mode. The duration of the pulse train was 1 msec. The deflecting mirror 2" directed the light beam to an optical system consisting of the spherical lenses 3" and 4" and the cylindrical lens 5", which converted the beam to planar (of width 80 cm and thickness 1 mm). The illuminated region of the two-phase flow and of the model 13 was recorded by means of the objectives 6' and 7' and the camera 8'.

The supersonic gas stream was generated by means of the two-dimensional shaped nozzle 12. The gas parameters in the settling chamber were: pressure $p_0 = 8.5 \cdot 10^5$ Pa, temperature $T_0 = 260°K$, Mach number at the nozzle rim $M_\infty = 3$. The throat dimension was 5 × 20 mm. The test models (cylinder, wedge, sphere, and cone), made of bronze or stainless steel, were set up near the end of the nozzle. Optical windows were provided for the optical measurements — two side windows and a window on top. In the experiments we used a wide range of solid particles varying considerably in material density $\rho$ and diameter $d_{av}$: bronze particles with $d_{av} = 100$ μm; particles of plastic with $\rho = 8.6$ g/cm$^3$; of aluminum with $d_{av} = 200$ μm; $\rho = 1.2$ g/cm$^3$; and of lycopodium with $d_{av} = 15$ μm, $\rho = 2.7$ g/cm$^3$, $d_{av} = 25$ μm, $\rho = 0.5$ g/cm$^3$. A special dust-producing device 14 was used to inject the particles into the gas stream at a distance of 300 mm ahead of the throat. The experimental equipment and the diagnostic apparatus have been described in more detail in [7, 8].

2. To observe the general picture of two-phase flow over bodies and elucidate the main physical laws of the process, the first tests were devoted to flow visualization using bodies of various geometry and injecting particles of different kinds into the flow.

Figures 2 and 3 show typical photographs obtained in flow visualization in scattered and transmitted laser light. The scattered light photographs (Fig. 2 uses the laser knife-edge method) illustrate the trajectory of particles (1 is a cylinder, with bronze particles, $d_{av} = 80$ μm, $\rho = 8.6$ g/cm$^3$; and 2 is a sphere, with aluminum particles, $d_{av} = 16$ μm, $\rho = 2.7$ g/cm$^3$; 3 is a cylinder, bronze particles, and 4 is a cylinder, mounted parallel to the flow with aluminum particles). The reflected particles are clearly seen. Some of them, depending on the shape of the body nose, have an angle of reflection close to the angle of incidence. Following reflection and subsequent stagnation by the oppositely directed flow, these particles reverse their direction of motion, and, after accelerating in the direction of the body, impinge on it afresh. Let L be the recoil length, defined as the maximum distance to which a particle departs on reflection from the body, and let $a$ be the distance of the

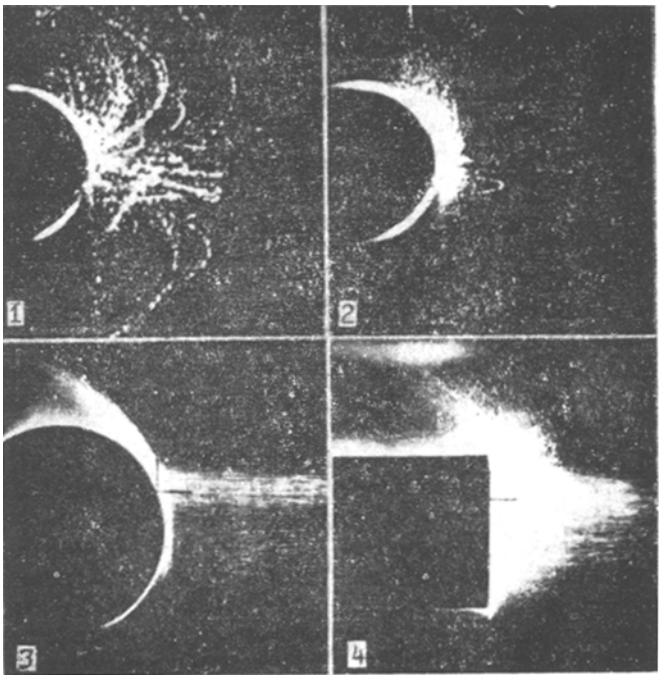

Fig. 2

bow shock from the body surface (standoff distance). As can be seen from Fig. 2, depending on the particle parameters $d_{av}$ and $\rho$, the value of L can be either less than $a$, or greater than $a$, i.e., in the second case the particles on reflection intersect the shock front.

The presence of particles which can collide repeatedly with the body with a sequentially reduced recoil length L leads to their clustering near the body nose. A zone of increased concentration of dispersed phase is formed in which there is a strong interaction between incident and reflected particles. Figure 2 (frames 3 and 4) shows that the size of this zone increases with increase of the mass content of particles in the flow.

Figure 3 shows typical shadowgrams illustrating the perturbation of the wave structure near a cylinder mounted parallel to the flow, with various particles injected into the flow (1 — flow with no particles; 2 — with lycopodium particles of $d_{av}$ = 25 μm; $\rho$ = 0.5 g/cm$^3$ ; 3-5 — with plastic particles of $d_{av}$ = 200 μm, $\rho$ = 1.2 g/cm$^3$; 1-4 — single-exposure photographs and 5 has three exposures). One can clearly see the local shock waves formed near particles in supersonic flow, and also the nature of the change in the structure of the bow shock due to the presence of the particles. For comparison Fig. 3 also shows a photograph of flow of clean air over the bodies. The incident stream Mach number is $M_\infty$ = 2.6.

From analysis of the large volume of experimental data one can note the following laws connected with the influence of particles on the structure of the bow shock wave. The nature of the change in the wave structure, and therefore, its basic characteristics depend both on the shape of the body (blunted or sharp nose), and on the particle parameters: size, concentration, etc. In flow over bodies with blunted noses (sphere or cylinder mounted parallel to the flow) and with rather fine particles injected into the stream (of aluminum and lycopodium) the influence of the disperse phase on the bow shock structure begins to appear when the volume concentration of particles m > m* = 0.5-1%. On the shadowgrams (see, e.g., Fig. 3, frame 2) this phenomenon shows up as a change in the shock standoff distance and a change in shock shape.

It was noted in [9, 10] that one can neglect the interaction between particles and their influence on the gas if the volume concentration of the disperse phase m < 0.5-1% or the ratio $l/d > 5$, where $l$ is the mean distance between particles in the flow and d is their diameter. In this case one has the "isolated particle" flow regime [11]. For m $\geqslant$1% ($l/d < 5$) we begin to see effects of deformation, leading to a substantial change in the gas parameters compared with the "pure" flow. This leads to a change in the incident flow Mach number, and

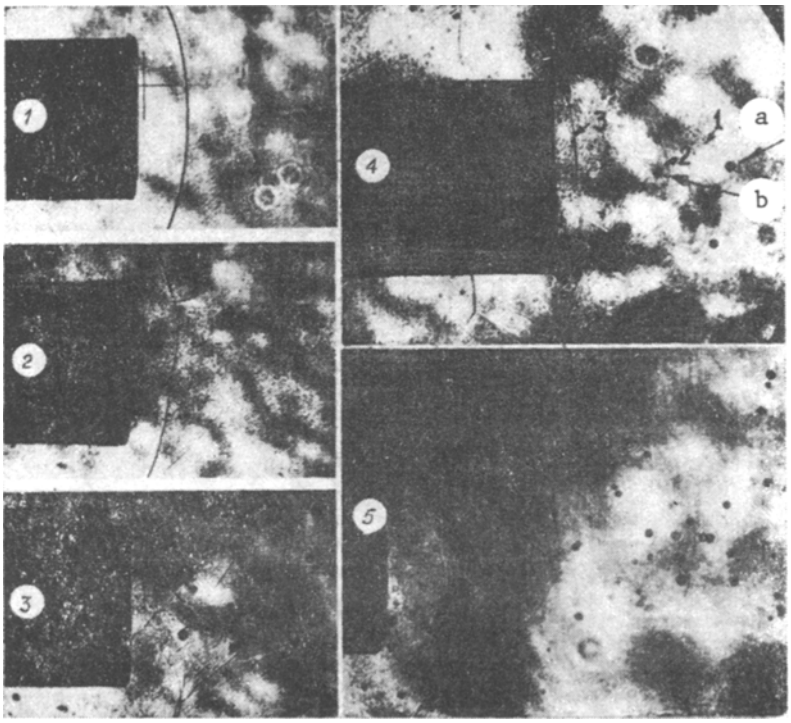


Fig. 3

therefore, to a change in the location of the bow shock. The value m* = 1%, determined in tests of flow over bodies, agrees satisfactorily with the prior experimental data [7, 10], obtained in investigation of two-phase flow in nozzles. The distortion of the bow shock observed in some cases (Fig. 3, frame 2) may be associated with a varying particle concentration over the section, or with the formation of the zone of increased particle concentration noted above ahead of the body, leading to a real change in the forebody geometry and therefore in the shape of the bow shock.

In flow over blunt bodies of a gas stream with the coarsest particles of plastic ($d_{av}$ = 200 μm, $\rho$ = 1.2 g/cm$^3$) and bronze ($d_{av}$ = 100 μm, $\rho$ = 8.7 g/cm$^3$) the nature of the variation of the wave structure changes markedly. Even for a low particle concentration ($m \ll 1\%$) one observes a strong perturbation of the bow shock. These perturbations take the form of conical shocks with a large vertex angle, and with particles at the apex. This can easily be seen in the flow over a cylinder mounted parallel to the stream (Fig. 3, frames 4 and 5), where one can speak of breakdown of the normal shock typical of the "pure" gas flow. This effect was not observed in flow over sharp bodies. One can therefore postulate that a special role in its formation is played by reflected particles which, after moving against the stream, intersect the shock wave and exit into the supersonic region. To confirm this hypothesis we made multiexposure shadowgrams, and also conducted additional tests with a hollow cylinder.

Figure 3 (frame 5) shows a three-exposure shadow photograph in which one can trace the dynamics of the perturbation of the bow shock with time. We consider a particle marked on the photograph by arrows. One can see that it is located at the apex of the conical shock with a large vertex angle, as mentioned above. Since the time between exposures is constant, 20 μsec, it is evident that this particle is reflected from the body, since its velocity changes rapidly as it departs from the body, as a result of deceleration by the counter stream.

Figure 4 (1 — shock wave; and 2 — hollow cylinder) shows shadowgrams obtained in flow over a hollow cylinder of a two-phase stream with different concentrations of plastic particles ($d_{av}$ = 200 μm, $\rho$ = 1.2 g/cm$^3$). In this case the probability of reflection of particles is very low, and the main role is played by the interaction of the incident particles with the shock wave. It can be seen that the nature of the perturbation of the bow shock differs appreciably from the case of flow over a solid cylinder, and takes the form of local perturbations of the bow shock where it is intersected by the incident particles. The character-

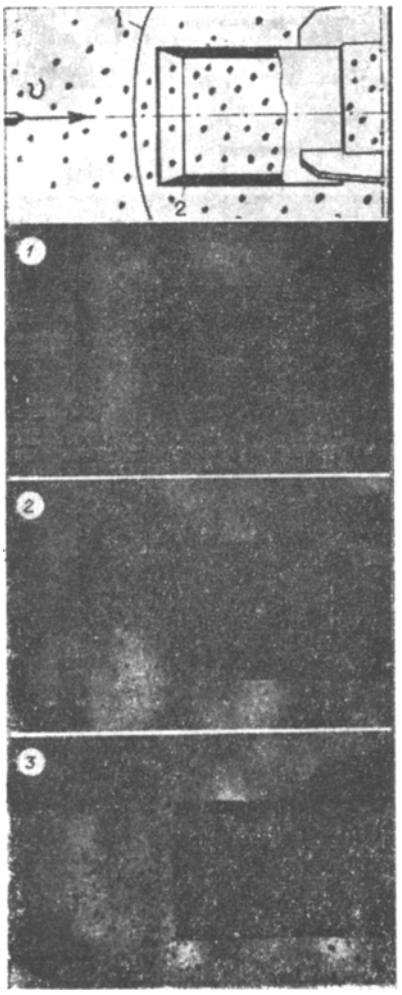


Fig. 4

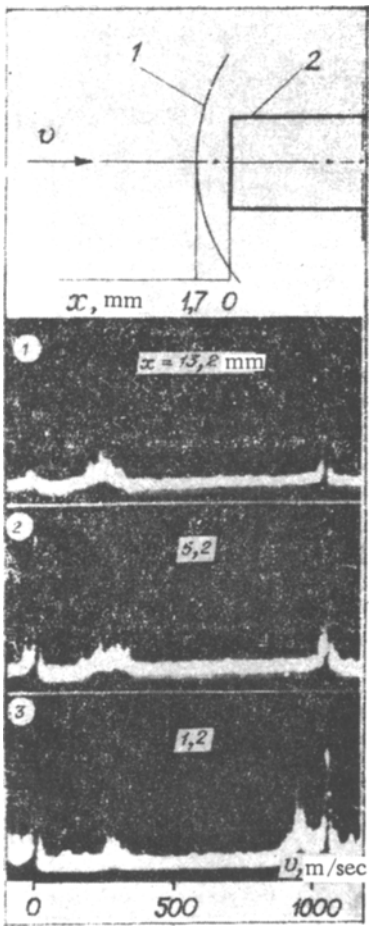


Fig. 5

istic size of these perturbations is on the order of the transonic region of the shock wave layer formed about a particle in supersonic flow [11]. Even at high concentration (Fig. 4, frames 2 and 3) one can distinguish the bow shock shape characteristic of this type of body. Here we observed no perturbations in the form of conical shocks with large vertex angle, as recorded in the flow over blunt bodies.

It is known [7, 9] that the nature of the change in the velocity of motion of particles in a gas stream is determined by the relaxation time $\tau = \rho_p d/[C_x \rho (v - v_p)]$, where $\rho_p$, $v_p$ and d are the material density and the particle velocity and diameter; $C_x$ is the aerodynamic drag coefficient; and $\rho$ and v are the gas density and velocity. Therefore, the recoil length of particles L is determined both by the nature of the collision with the body surface, and by the time $\tau$. For a specific initial recoil velocity the value of L increases with increase of $\rho_p$ and d, may exceed $a$ for a certain value of $\tau$. This is just the thing that can explain the different nature of the action of the particles used in the experiment on the wave structure in the flow over blunt bodies. For the aluminum and lycopodium particles $L < a$ and the main role is played by effects associated with the influence of the particles on the parameters of the incident gas stream, and also with the formation of the increased particle concentration zone at the body nose. These factors are important only for $m > 1\%$. For $L > a$, independently of concentration, the reflected particles lead to the appearance of a new effect responsible for perturbing the bow shock structure, as occurs when particles of plastic and bronze are injected into the flow. That these particles exit into the supersonic zone on reflection is confirmed by observation of their trajectories near the body (Fig. 2, frame 1), and also by data obtained with the aid of the LDVM.

Figure 5 shows typical oscillograms (1 — shock wave; 2 — cylinder), obtained during measurement of velocity of plastic particles at points at different distances from the surface

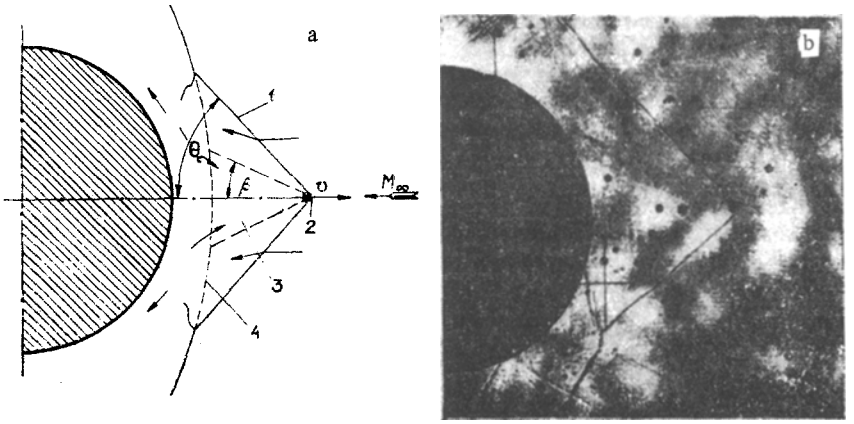


Fig. 6

of a cylinder mounted parallel to the flow. The signal on the left corresponds to the incident particles, and that on the right corresponds to the reflected particles. It can be seen that at x = 1.2 mm, $v_{p1}$ = 270 m/sec, $v_{p2}$ = 100 m/sec. As the distance from the body increases, the velocity of reflected particles, in contrast with that of the incident particles, varies rather rapidly, and at x = 5.2 mm it is $v_{p2}$ = 10 m/sec. No reflected particle are recorded at x = 13.2 mm. From the measured data one can estimate the size of the zone in which reflected particles are present. For plastic particles we have L ≈ 6.5 mm, which agrees satisfactorily with measurements of L from trajectories of the motion, and is greater by a factor of about 3.5 than the shock standoff distance in the flow unperturbed by particles.

3. It is evident, that, in comparison with the incident particles, the process of interaction of reflected particles with the shock wave is more complex. When a reflected particle passes through the front of the shock the high pressure from the subsonic region can be transmitted through the particle wake into the supersonic part of the flow, leading to the appearance of a complex structure in the wake behind the particle.

We now consider a simplified scheme for this phenomenon, depicted in Fig. 6a (1 — shock; 2 — reflected particle; 3 — region of entrained gas; and 4 — original shock position). As indicated in the shadow photographs (Fig. 6b), the nature of the perturbation introduced by this kind of particle is formation of a nearly conical shock propagating upstream along with the reflected particle. Here the cone vertex angle is considerably larger than the appropriate Mach angle. The formation of this shock can be explained as the formation behind the particle of a local gas region with increased pressure ($p_k > p_\infty$), transmitted from the subsonic part, where the pressure $p_2 > p_k$, through the particle wake. From the shape of this shock one can postulate that this region has the form of a cone whose apex contains the particle. Knowing the velocity of the reflected particle from the experiment, one can estimate the pressure $p_k$, and therefore, also determine the shock angle θ.

We shall assume that the velocity of motion of this "gas cone" is that of the particle motion. Then the pressure in it can be estimated from the equation of balance of the total energy for a jet [12], considering that the motion of the gas in the wake behind the particle is due to the pressure drop $p_2 - p_k$: $p_k = p_2\{1 - [(k-1)/(k+1)]\lambda^2\}^{k/(k-1)}$, where k = 1.4; $\lambda = (|v_p| + |v_2|)\Big/\left(a_2\sqrt{\frac{2}{(k+1)}}\right)$.

If we assume that this pressure is also found on the surface of the "gas cone," we can determine its semi-vertex angle β, using the relation [13] $(p_k - p_1)/0.7pM^2 = (0.0016 + 0.002M_k^{-2})\beta^{1,7}$. Here one must evaluate $M_k$ from the relative velocity and the sound speed ahead of the shock wave: $M_k = (|v_k| + |v_\infty|)/a_\infty$. Knowing β and $M_k$, one can determine the semivertex angle θ for the shock, using, for example, the computational grid presented in [13]. The calculations were performed for the following flow parameters, corresponding to the conditions under which the experimental data were taken: stagnation pressure $p_0 = 8.5 \cdot 10^5$ Pa, stagnation temperature $T_0$ = 260°K, and incident stream Mach number $M_\infty$ = 2.6. Here $p_\infty = 0.45 \cdot 10$ Pa, $T_\infty$ = 113°K, $v_\infty$ = 550 m/sec, $p_2 = 3.4 \cdot 10^5$ Pa, $T_2$ = 250°K, $v_2$ = 160 m/sec, $M_2$ = 0.5. The results of calculations of β and θ for three values of particle velocity $v_{p1}$ =

TABLE 1

| $v_p$, m/sec | $\beta°$ | $\theta°$ | $\gamma°$ |
|---|---|---|---|
| 50 | 36 | 47 | 21 |
| 100 | 29 | 39 | 19,5 |
| 150 | 22 | 32 | 17,5 |

50 m/sec, $v_{p2}$ = 100 m/sec and $v_{p3}$ = 150 m/sec are shown in Table 1. For comparison Table 1 also shows values of Mach angle $\gamma$, computed from the relative velocity of the reflected particle $|v_p| + |v_\infty|$ and $M_\infty$.

We compare these data with the results of the experiment. The shadow photographs give values of the shock semivertex angle $\theta$ for a reflected particle located at the given point from the body L. From the laser-Doppler measurement data one can find the average velocity of the reflected particles at the given point. For this purpose we can also use the multiexposure shadow photographs (Fig. 3, frame 5) to determine $v_p$ and $\theta$ simultaneously for a given particle.

Comparison of the experimentally determined and the calculated values of $v_p$ and $\theta$ shows them to be in satisfactory agreement. For example, for a particle located at the apex of a conical shock (Fig. 6b) we have L = 4 mm, $v_p$ = 60 m/sec, $\theta$ = 43°, which are close to the values of v and $\theta$ given in Table 1.

Thus, in supersonic two-phase flow over blunt bodies an important part is played by perturbation of the bow shock associated with the presence of reflected particles, if their recoil length $L > a$. With the model examined above one can qualitatively explain the physical mechanism of this phenomenon and evaluate the parameters of the cone shock at the initial stage of the process where an individual particle passes out into the supersonic region. With increased distance of the reflected particle from the body its link to the subsonic region will be reduced, and at some value we begin the process of restoring the original bow shock shape. Figure 3 (frame 4) illustrates this situation, when supersonic flow is formed in the region behind the reflected particle $a$ with a cone shock 1. We can readily see the presence of a local shock 2 about the incident particle b, and also the appearance of a bow shock 3 ahead of the body.

An analogous phenomenon is observed in supersonic flow over two bodies of comparable size, one of them mounted in the wake of the other. As was show, for example, in [14], for a certain distance between the two the flow readjusts from a regime with a separated region to a regime with a bow shock ahead of the second body. However, in the conditions of our experiments it is considerably more difficult to analyze the process because it is unsteady. For high concentration, when the repetition time between the two reflected particles $\tau_w < \tau_r$, the time for recovery of the bow shock, there is breakdown of the normal shock typical of blunt bodies and formation of a certain transition flow region of dimension ~L ahead of the body, consisting of a series of conical shocks. This phenomenon can lead to a substantial readjustment of the flow field near the body and to a change in its aerodynamic characteristics. To explain the mechanism of these processes requires further theoretical and experimental investigations. It is important, in particular, to analyze the possibility of change in the drag of bodies in supersonic flight due to particles being blown ahead. If the time between successive flights of two particles is less than the flow recovery time, then the normal shock could be continuously transformed into a cone, which must lead, as when spikes are present [15], to reduced frontal drag of blunt bodies.

## LITERATURE CITED


1. G. A. Saltanov, Supersonic Two-Phase Flow [in Russian], Vysshaya Shkola, Minsk (1972).
2. J. H. Spurk and N. Gerber, "Dust collection efficiency for power-law bodies in hypersonic flight," AIAA J., 10, No. 6 (1972).
3. R. F. Probstein and F. Fassio, "Dusty hypersonic flows," AIAA J., 8, No. 4 (1970).
4. G. D. Waldman and W. G. Reinecke, "Particle trajectories, heating and breakup in hypersonic shock layer," AIAA J., 9, No. 6 (1971).
5. B. A. Balanin and V. V. Zlobin, "Experimental investigation of the aerodynamic drag of simple bodies in two-phase flow," Izv. Akad. Nauk SSSR, Mekh. Zhidk. Gaza, No. 3 (1979).

6. L. E. Dunbar, J. F. Courtney, and L. D. McMillen, "Heating augmentation in erosive hypersonic environments," AIAA J., 13, No. 7 (1975).
7. N. N. Yanenko, R. I. Solukhin, A. N. Napyrin, and V. M. Fomin, Supersonic Two-Phase Flow with Particles Not in Velocity Equilibrium [in Russian], Nauka, Novosibirsk (1980).
8. V. F. Klimkin, A. N. Papyrin, and R. I. Soloukhin, Optical Methods for Recording High-Speed Processes [in Russian], Nauka, Novosibirsk (1980).
9. S. Sou, Hydrodynamics of Multiphase Systems [Russian translation], Mir, Moscow (1971).
10. A. P. Alkhimov, A. N. Papyrin, et al., "Theoretical and experimental investigation of the motion of a gas mixture with solid particles in a Laval nozzle," Chisl. Metody. Mekh. Sil. Sredy, 9, No. 2 (1978).
11. V. I. Blagosklonov, V. M. Kuznetsov, et al., "The interaction of hypersonic multiphase flows," Zh. Prikl. Mekh. Tekh. Fiz., No. 9 (1979).
12. L. G. Loitsyanskii, Mechanics of Liquids and Gases [Russian translation], Nauka, Moscow (1970).
13. N. F. Krasnov, Aerodynamics of Bodies of Revolution [in Russian], Mashinostroenie, Moscow (1964).
14. V. S. Khlebnikov, "Readjustment of the flow between a pair of bodies of which one is located in the wake of the other in supersonic flow," Uch. Zap. Tsentr. Aero. Gidr. Inst., 7, No. 3 (1976).
15. P. Chen, Control of Flow Separation [Russian translation], Mir, Moscow (1979).

# THE QUASI-TWO-DIMENSIONAL APPROXIMATION IN THE PROBLEM OF STATIONARY SUBSONIC FLOW OVER A THREE-DIMENSIONAL ANNULAR BLADE ROW

V. P. Ryabchenko

UDC 532.5:621.22

Subsonic flows in axial compressors are usually studied on the basis of a plane or axisymmetric theory of blade rows. Results obtained using these approximations do not give an adequate description of three-dimensional flow, however. In a number of reports [1-3] attempts are made to determine the corrections to these approximate theories allowing for the three-dimensional character of the flow under certain limiting assumptions. Irrotational flow over an annular blade row was analyzed in [1], the inverse problem of blade-row theory was solved in [2], and in [3] a two-dimensional approximation was obtained from a three-dimensional theory based on the use of an acceleration potential. Nevertheless, there is no clear procedure for estimating the relative contributions of the effects which are not taken into account by the plane theory. In particular, allowance for the variation of the Mach number over the height of a blade can prove important for modern compressors.

In the present report a two-dimensional approximation is obtained from the three-dimensional theory of a nonbearing surface in the limiting case of an infinitely large number of blades and a hub ratio close to one.

1. We shall consider the subsonic adiabatic flow of an ideal gas through one blade row rotating with a constant angular velocity $\omega$ in an infinite channel between two coaxial cylinders (see Fig. 1). The absolute motion of the gas near this annular blade row will be taken as potential. We introduce a moving coordinate system Oxyz, which rotates about the axis of the cylinders with an angular velocity $\omega$ and the x axis of which coincides with the axis of rotation. In this coordinate system the Cauchy—Lagrange integral can be written in the form [4]

$$\frac{\partial' \varphi}{\partial t} + \frac{1}{2}\left[\left(\frac{\partial \varphi}{\partial x}\right)^2 + \left(\frac{\partial \varphi}{\partial y}\right)^2 + \left(\frac{\partial \varphi}{\partial z}\right)^2\right] - \omega z \frac{\partial \varphi}{\partial y} + \omega y \frac{\partial \varphi}{\partial z} + P = F(t), \tag{1.1}$$

where $\varphi$ is the velocity potential of the absolute motion of the gas; a prime denotes time differentiation in the moving coordinate system; F(t) is an arbitrary function of time;

Novosibirsk. Translated from Zhurnal Prikladnoi Mekhaniki i Tekhnicheskoi Fiziki, No. 2, pp. 74-80, March-April, 1982. Original article submitted March 4, 1981.

 0021-8944/82/2302-0226$07.50 